Letter

Fingerprints of composite fermion Lambda levels in scanning tunneling microscopy

Songyang Pu,[1,2,*] Ajit C. Balram,[3,4,*] Yuwen Hu,[5] Yen-Chen Tsui,[5] Minhao He,[5] Nicolas Regnault,[6,5] Michael P. Zaletel,[7] Ali Yazdani,[5] and Zlatko Papić[1]

[1]*School of Physics and Astronomy, University of Leeds, Leeds LS2 9JT, United Kingdom*
[2]*Department of Physics and Astronomy, University of Tennessee, Knoxville, Tennessee 37996, USA*
[3]*Institute of Mathematical Sciences, CIT Campus, Chennai 600113, India*
[4]*Homi Bhabha National Institute, Training School Complex, Anushaktinagar, Mumbai 400094, India*
[5]*Department of Physics, Princeton University, Princeton, New Jersey 08544, USA*
[6]*Laboratoire de Physique de l'Ecole normale supérieure, ENS, Université PSL, CNRS, Sorbonne Université, Paris 75005, France*
[7]*Department of Physics, University of California, Berkeley, California 94720, USA*

(Received 13 December 2023; accepted 29 July 2024; published 14 August 2024)

A composite fermion (CF) is a topological quasiparticle that emerges from a nonperturbative attachment of vortices to electrons in strongly correlated two-dimensional materials. Similar to noninteracting fermions that form Landau levels in a magnetic field, CFs can fill analogous "Lambda" levels, giving rise to the fractional quantum Hall (FQH) effect of electrons. Here, we show that Lambda levels can be directly visualized through the characteristic peak structure in the signal obtained via spectroscopy with scanning tunneling microscopy (STM) on a FQH state. Complementary to transport, which probes the low-energy properties of CFs, we show that *high-energy* features in STM spectra can be interpreted in terms of Lambda levels. We numerically demonstrate that STM spectra can be accurately modeled using Jain's CF theory. Our results show that STM provides a powerful tool for revealing the anatomy of FQH states and identifying physics beyond the noninteracting CF paradigm.

DOI: 10.1103/PhysRevB.110.L081107

Introduction. Fractional quantum Hall (FQH) phases [1] of matter possess nonlocal order which gives rise to topologically quantized Hall conductance, dissipationless boundary modes, and emergent quasiparticle excitations that are distinct from fermions or bosons [2–5]. While some of these properties have been successfully accessed via transport [1] and interferometry [6,7] measurements, recent advances in scanning tunneling microscopy (STM) [8–11] have opened a new window to directly probe FQH states at much higher energies than in the past. The sensitivity of early spectroscopy experiments on GaAs materials [12–16] was heavily constrained by the two-dimensional electron gas residing deep inside the semiconductor heterostructures. These limitations have recently been lifted in two important ways: by utilizing ultraclean graphene materials, which host FQH states atomically close to the vacuum [17–24], and by STM tip preparation [10,11] that allows performing noninvasive imaging of FQH states. Moreover, in samples with a few defects, STM was used to directly probe the spatial structure of the Landau orbits [25], and in materials such as bismuth, it was used to visualize lattice-symmetry-broken ground states [26].

In light of these developments, a question arises: what does the STM, performed on a FQH state, actually measure? A textbook answer is that STM probes the local density of states (LDOS) for the injection or removal of an electron from the system. However, the underlying quasiparticles of FQH states are *composite fermions* (CFs) [27]—electrons bound to vortices. Due to the nonperturbative nature of vortex attachment, predicting the measured STM signal becomes a highly nontrivial task, as anticipated in early theoretical works [28–30]. At low electron densities insufficient to form a FQH state, the LDOS can be analytically computed [31–33] and shown to consist of a series of peaks at energies given by the Haldane pseudopotentials [34], providing a useful characterization of the relevant energy scales in a Landau level (LL) [10,16]. By contrast, the understanding of the detailed structure of the STM spectra in the FQH regime has so far been lacking. For Jain states at electron filling factors $\nu = 1/3, 2/5, 3/7$, etc., it was previously argued that a single hole and electron excitations have finite overlap on a tightly bound state of multiple CFs, which should manifest as a resonance in the LDOS [35]. However, recent high-resolution experiments on Bernal stacked bilayer graphene have reported *multiple* sharp resonances for various FQH states realized in this system [11]. Moreover, the observed pattern of resonances displayed an intriguing asymmetry between the addition and removal of an electron.

In this Letter, we show that the LDOS, measured by scanning tunneling spectroscopy on a FQH state, consists of multiple peaks that can be naturally interpreted as CF

*These authors contributed equally to this work.

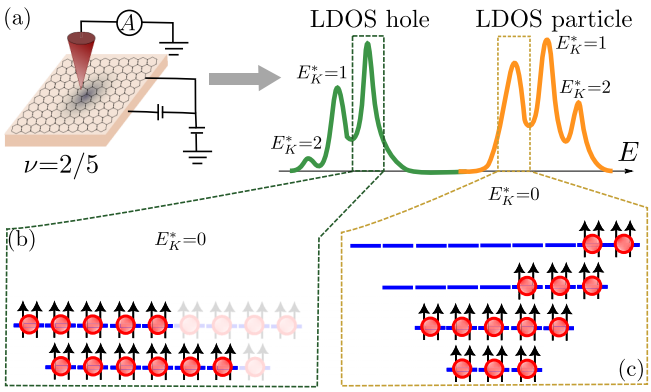

FIG. 1. (a) Schematic of the STM probe of a $\nu = 2/5$ FQH state and measured signal on the hole and particle sides. (b) and (c) The signal peaks are fingerprints of CF Landau levels. The first peak on the hole side corresponds to the $E_K^* = 0$ state where five CF holes are in the lowest two ΛLs, as shown (see text for the definition of E_K^*). On the particle side, the $E_K^* = 0$ state is obtained when one electron is added, corresponding to five CF particles that occupy higher, $n \geqslant 2$, ΛLs.

"Lambda levels" (ΛLs)—analogs of LLs of electrons [36]; see Fig. 1 for a schematic summary. We develop an efficient method for extracting LDOS spectra of FQH states belonging to the Jain sequence using CF wave functions, and we confirm its accuracy against exact diagonalization simulations. The interpretation of LDOS spectra in terms of ΛLs explains the strong asymmetry in the numerically computed spectra for the addition vs removal of an electron, which relates to the well-known asymmetry between CF quasiparticles and quasiholes. Implications for future experiments and potential uses of STM as a probe of new FQH states extending beyond the noninteracting CF paradigm are also discussed.

CF model for LDOS. We consider tunneling an electron into a FQH ground state $|\Omega\rangle$ with N electrons. We assume the electrons are on the surface of a sphere, with a Dirac monopole at the center carrying $2Q$ flux quanta [34]. The radius of the sphere is $R = \sqrt{Q}\ell$, where $\ell = \sqrt{\hbar c/eB}$ is the magnetic length at magnetic field B. We consider Coulomb interaction for simplicity and express all energies in units of $E_C \equiv e^2/\varepsilon\ell$. We will focus on uniform FQH states residing in the lowest LL (LLL), with orbital angular momentum $L = 0$. The electron is tunneled into the north pole, which is defined by the LL orbital with $L_z = Q$, and the corresponding energy-resolved LDOS is [37,38]

$$\mathrm{LDOS}(E, L_z = Q) = \sum_n \delta(E - E_n^-)|\langle n|c_{-Q}|\Omega\rangle|^2 + \sum_n \delta(E - E_n^+)|\langle n|c_Q^\dagger|\Omega\rangle|^2, \quad (1)$$

where c and $c^\dagger$ are the electron annihilation and creation operators and n runs over all eigenstates with energy $E_n^\pm$ for $N\pm1$ electrons at the same flux $2Q$ as in the ground state. For convenience, we will always assume that the tunneling process involves removing an electron from the south pole or adding it to the north pole, resulting in a state with $L = L_z = Q$. This can be assumed without any loss of generality since the FQH ground state is uniform. Henceforth, we will suppress the L_z dependence.

In principle, one could evaluate LDOS in Eq. (1) by brute force, obtaining all the eigenstates via exact diagonalization. However, this severely limits the accessible system sizes, amplifying the finite-size effects; furthermore, it sheds little light on the physics behind any of the observed LDOS features. We turn to CF theory [27,36] to overcome these obstacles. In CF theory [27,36], Jain states at fillings $\nu = n/(2pn\pm1)$ are mapped into integer quantum Hall (IQH) states of CFs carrying $2p$ vortices and filling n ΛLs in a reduced effective flux of $2Q^* = 2Q - 2p(N-1)$ [all CF quantities are marked by a superscript asterisk (*)]. An example of $\nu = 2/5$ is given in Fig. 1(b), with the shaded holes also filled. The Jain wave functions for these FQH states are given by $\Psi_{\nu=n/(2pn\pm1)} = \mathcal{P}_{\mathrm{LLL}}\Phi_{\pm n}\Phi_1^{2p}$, where Φ_n is the Slater determinant wave function of n filled LLs ($\Phi_{-n} = [\Phi_n]^*$) and $\mathcal{P}_{\mathrm{LLL}}$ is the projection operator to the LLL. From here on in, for convenience, we shall restrict our discussion to the $n/(2n+1)$ Jain states.

In CF theory, the removal of an electron from an FQH ground state (i.e., creating a hole excitation) is equivalent to creating $2n+1$ holes in the lowest n ΛLs ($n = 0, 1, 2, \ldots$), as shown in Fig. 1(b). We refer to the "CF space" as the Hilbert space of $2n+1$ holes with $L = L_z = Q$ in the lowest n ΛLs. While the dimension of the Hilbert space of $N-1$ electrons in the LLL with $2Q$ fluxes and $L = L_z = Q$ grows exponentially with N, the dimension of the CF space is a constant (up to a linear dependency for small N): for example, at $\nu = 1/3$ there is a unique state, at $\nu = 2/5$ there are 3 states, at $\nu = 3/7$ there are 27 states, etc. This makes the diagonalizations in CF space much more efficient than in the full LLL space. Furthermore, CF theory provides explicit wave functions for the basis states that span the CF space, which we write as $\Psi^{-,i}_{\nu=n/(2n+1)} = \mathcal{P}_{\mathrm{LLL}}\Phi_n^{-,i}\Phi_1^2$. Here, $\Phi_n^{-,i}$ denote Slater determinants, indexed by i, of $N-1$ particles, which is equivalent to $2n+1$ holes in the lowest n ΛLs at flux $2Q^* = 2Q - 2(N-2)$, with total angular momentum $L = L_z = Q$. These basis states, however, are not orthogonal, and we perform CF diagonalization (CFD) [39] to obtain orthonormal states in the CF space, as detailed in the Supplemental Material (SM) [40].

Similarly, we consider adding one electron at the north pole. This is equivalent to creating $2n+1$ particles in the $m \geqslant n$ ΛLs, as shown in Fig. 1(c). The CF space is now spanned by states of the form $\Psi^{+,i}_{\nu=n/(2n+1)} = \mathcal{P}_{\mathrm{LLL}}\Phi_n^{+,i}\Phi_1^2$, where $\Phi_n^{+,i}$ are Slater determinants for $(2n+1)$ particles in the ΛLs with index $\geqslant n$ at flux $2Q^* = 2Q - 2N$ with angular momentum $L = L_z = Q$. Naively, one might think the dimension of the CF space for adding one electron would be infinite, as the ΛLs do not have an upper bound. Nevertheless, this is not true because the CF space is still a subspace of the original Hilbert space of $N+1$ electrons in the LLL. This implies that the basis states of the CF space are not linearly independent. We classify the CF basis states by their effective kinetic energy, $E_K^* = \sum_{l=1}^{2n+1}(n_l - n) - E_0$, where n_l is the ΛL index of the lth particle and E_0 is the minimal value of $\sum_{l=1}^{2n+1}(n_l - n)$ in the $L_z = Q$ sector. For instance, $E_0 = 7$ for the configuration shown in Fig. 1(c). The CF kinetic energy is expressed in units of $\hbar\omega_c^*$, where ω_c^* is the CF cyclotron frequency. In practice, we carry out CFD in the CF subspace obtained by imposing

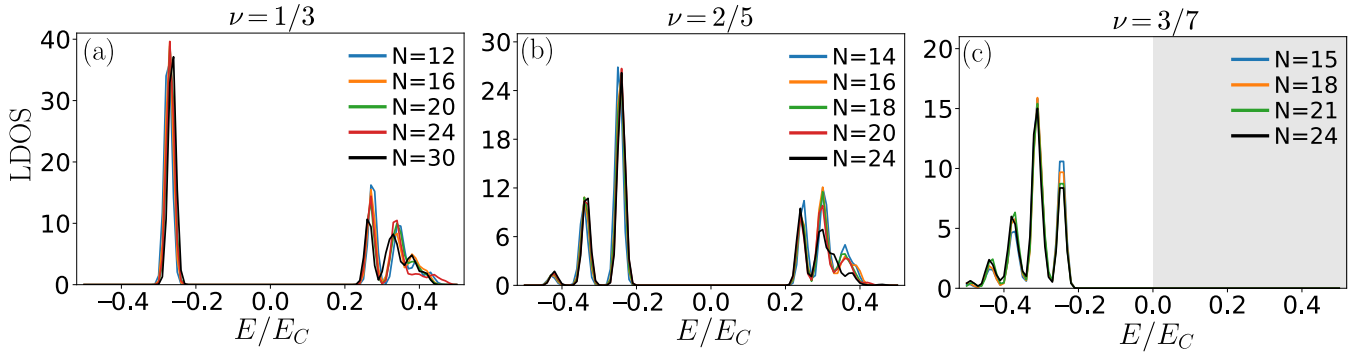

FIG. 2. LDOS for FQH states at $\nu = 1/3$, 2/5, and 3/7, obtained using CF theory reveals distinctive peak structures on the hole and particle sides. We include the full CF space for the hole side and do a truncation $E_K^* \leqslant 2$ for the particle side. For the hole side, the data are well converged across the range of systems shown in the legend. The computation of the particle side of the LDOS is computationally intensive due to the unbounded growth of CF space; hence, convergence was achieved only at $\nu = 1/3$, 2/5, and thus, the particle side is omitted for 3/7. All energies are quoted in units of $E_C = e^2/\varepsilon\ell$.

an upper cutoff on E_K^* and checking for convergence as this cutoff is increased. Similarly, E_K^* is defined for the hole side with the replacement $n_l - n \to n - n_l$ [$E_0 = 1$ for the state shown in Fig. 1(b)].

We refer to the orthonormal states obtained from CFD as $|\alpha_n^{\pm}\rangle$ for adding and removing electrons, with the corresponding energy eigenvalues $E_n^{\pm}$, and define their corresponding overlaps with the electron and hole excitations as $\eta_n^+ = \langle\alpha_n^+|c_Q^\dagger|\Omega\rangle$ and $\eta_n^- = \langle\alpha_n^-|c_{-Q}|\Omega\rangle$, where $|\alpha_n^{\pm}\rangle$, $c_Q^\dagger|\Omega\rangle$, and $c_{-Q}|\Omega\rangle$ are all normalized to unity. Following Eq. (1), we define the CF approximation to the LDOS as

$$\mathrm{LDOS}(E) = \sum_n [\delta(E - E_n^-)|\eta_n^-|^2 + \delta(E - E_n^+)|\eta_n^+|^2]. \quad (2)$$

When plotting the LDOS, we express the energy relative to the chemical potential [29], including the appropriate electrostatic corrections as described in the SM [40]. We smear the δ function in Eq. (2) by a Gaussian of width $\sigma = 0.01E_C$ for easier visualization.

Results. We benchmarked the accuracy of the above CF computation of LDOS against exact diagonalization, finding excellent agreement within the system sizes accessible to both methods [40]. Although CF theory is known to successfully capture the ground states and low-lying excitations of Jain states [5,41], the accuracy of its LDOS approximation is, nevertheless, remarkable, given the smallness of the CF subspace and the high energies probed by electron tunneling into a FQH state.

Our main results are presented in Fig. 2, which shows the LDOS of FQH states at $\nu = 1/3$, 2/5, and 3/7 obtained with the CF method. These plots reveal characteristic sequences of LDOS peaks, e.g., one peak on the hole side for $\nu = 1/3$, three peaks on the particle side for $\nu = 1/3$, and three peaks on both the hole and particle sides for $\nu = 2/5$. These features are well converged across a range of system sizes; thus, they act as a universal "fingerprint" of each state, whose origin will be elucidated below. The LDOS is particularly well converged on the hole side, where we kept *all* basis states in the relevant CF space. On the particle side, the CF basis is unbounded, and we must enforce an explicit truncation to keep the computation tractable. The numerics become computationally more intensive as the number of CF basis states increases. In Fig. 2, we restrict the CF subspace to states with $E_K^* = 0$, 1, 2, which is sufficient to converge the particle side of LDOS at $\nu = 1/3$ and 2/5. For $\nu = 3/7$, however, this is insufficient to achieve convergence [40], and we do not show those data in Fig. 2.

To quantify the convergence of the CF calculation of LDOS, it is instructive to compute the total weight of states $c_{-Q}|\Omega\rangle$ and $c_Q^\dagger|\Omega\rangle$ in the CF space. If the total weight extrapolates to a value of the order of unity in the thermodynamic limit, we can be confident that the CF approximation is capturing the key spectral features associated with the addition or removal of an electron from a FQH state. These weights are shown in Fig. 3 for $\nu = 1/3$, 2/5, and 3/7 FQH states as a function of $1/N$. We see that the hole excitation fully resides within CF space, i.e., the total overlap of $c_{-Q}|\Omega\rangle$ on the CF basis is unity, and thus, the hole side of the LDOS is fully captured by the CF theory. On the other hand, due to the imposed truncation, the support of $c_Q^\dagger|\Omega\rangle$ in the truncated CF space is generally less than 1; thus, the particle side of LDOS is only partly captured by CF theory. In particular,

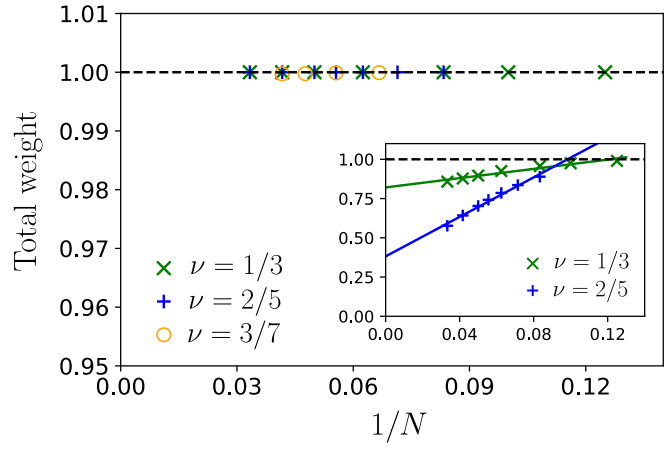

FIG. 3. Total weight $\sum_n |\eta_n^-|^2$, which represents the amplitude of $c_Q|\Omega\rangle$ in the CF space, is unity. This shows the hole state is fully contained within the CF space. Inset: Total weight $\sum_n |\eta_n^+|^2$, i.e., the amplitude of the state $c_Q^\dagger|\Omega\rangle$ in the CF space. Lines are linear fits through the data. These amplitudes can be increased by increasing the value of E_K^* at which we truncate (see text; we choose $E_K^* \leqslant 2$).

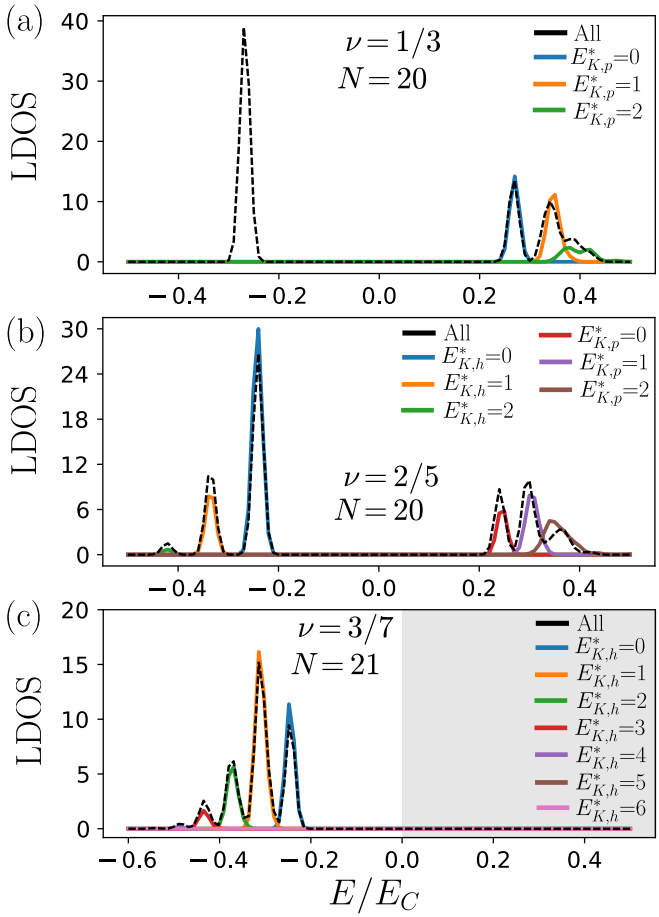

FIG. 4. Reconstructing the full LDOS by populating successive ΛLs with CFs in (a) the $\nu = 1/3$ and (b) 2/5 states with $N = 20$ electrons and (c) $\nu = 3/7$ with $N = 21$ electrons. The plots show the LDOS in different CF subspaces made up of states with a single value of E^*_K for the particle or hole side, indicated in the legend, after removing all contributions with lower values of E^*_K. Each LDOS peak is associated with a definite CF kinetic energy. Black dashed lines represent the full LDOS from Fig. 2.

in the thermodynamic limit, the truncated CF space captures about 80% of the electron excitation for $\nu = 1/3$ and 40% for $\nu = 2/5$. This number is expected to increase as we include more states with higher E^*_K.

We note that Ref. [35] computed overlaps similar to those in Fig. 3 by keeping only the unique state with the lowest E^*_K for both the particle and hole sides. By contrast, we include the full CF space on the hole side and a much bigger portion of CF space on the particle side. Nevertheless, even when restricting ourselves to the unique state with the lowest E^*_K, we find overlaps larger than those reported in Ref. [35]. Our results have been additionally verified by direct calculation in the Fock space for small N [42,43].

Relating LDOS peaks to ΛLs. The CF theory not only allows us to model LDOS quantitatively but also provides an understanding of the origins of peaks. We surmise that each peak can be associated with CF states that carry a well-defined value of the kinetic energy E^*_K. Numerical tests of this hypothesis are summarized in Fig. 4.

We first look at the simplest case: the hole side of $\nu = 1/3$. In this case, there is only a unique state in the CF space with $L = L_z = Q$, and it is clear from Fig. 2 that this CF state accounts for the only peak seen in this case [28]. Next, we consider the particle side of $\nu = 1/3$. We first look at the CF space of the $E^*_K = 0$ state, where there is only one state. We find that this state perfectly captures the lowest energy peak (blue line) on the particle side as shown in Fig. 4(a). Next, we go to the subspace made up of states with $E^*_K = 1$. Unlike in the IQH case, the states with different E^*_K are not naturally orthogonal to each other [39,41,44,45]. Therefore, we apply the Gram-Schmidt procedure to obtain a new basis for $E^*_K = 1$ which is orthogonal to the states with $E^*_K = 0$. We then carry out CFD on this new basis to obtain the LDOS [40]. After this, we find that the states in the resultant subspace perfectly capture the second peak (orange line) on the particle side. Finally, we repeat the above procedure for $E^*_K = 2$. While the peak height (green line) corresponding to this subspace does not perfectly match the third peak, the energy range where it occurs agrees well. We performed a similar analysis for $\nu = 2/5$ and the hole side of $\nu = 3/7$, finding similarly good agreement [see Figs. 4(b) and 4(c)].

Conclusions and discussion. We proposed that STM experiments, performed on FQH states belonging to the primary Jain sequence $\nu = n/(2n+1)$, can reveal sharp resonances associated with CF LLs. For sufficiently small $n \leqslant 3$, these features were shown to be robust across various system sizes, with good agreement between CF theory and exact numerics, despite the high energy of excitations probed in this setup.

A recent experiment on Bernal stacked bilayer graphene [11] reported three LDOS peaks for electronlike excitation for $\nu = 3/5$, which would correspond to our predicted $\nu = 2/5$ holelike excitation. In contrast, in the same experiment, $\nu = 2/3$ appeared to show not just one electronlike peak, but two, which our model would predict to have just one resonance. Future experiments would be required to make comparisons with our theoretical prediction. In particular, an important test for identifying the predicted ΛL peaks would be precise measurements of their field dependence. All the peaks in this work are interaction driven; hence, their positions should scale as $E_C \propto \sqrt{B}$. This would distinguish them, e.g., from additional features associated with the spin physics of CFs. Furthermore, for a direct comparison with experiment, it would be necessary to also include the effects of disorder and screening. Nevertheless, while these effects may impact the precise shape of LDOS spectra, we expect the correspondence between peaks and CF kinetic energy to continue to hold. We reserve detailed investigation of these effects for future work.

For larger n, i.e., filling factors approaching $\nu = 1/2$, the calculations presented above are expected to become significantly harder due to the faster growth of CF space. Moreover, the CF cyclotron energy becomes smaller as the CF Fermi liquid state at 1/2 is approached, implying that the identification of LDOS peaks with CF ΛLs may no longer be as straightforward as in Fig. 4 above. Due to the "aliasing" problem on the sphere [46], the study of such FQH states would also require larger system sizes, presenting an interesting challenge for theory.

Finally, our study opens up several interesting questions. Additional degrees of freedom such as spin, layer, valley, etc.,

will naturally give rise to richer LDOS spectra that could be studied using the present method. On the other hand, for higher-order CF states such as those at $\nu = 2/7,\ 2/9$ (where non-CF partonic features might be present [47]) and for states beyond the noninteracting CF paradigm, e.g., the paired $\nu = 5/2$ state, a different approach altogether may be needed to understand the LDOS. Consequently, we expect some violations of the peak structure identified above, which could serve as a diagnostic tool for unconventional physics extending beyond the standard CF theory at high energies [47,48].

Noted added. Recently, we became aware of a related work by Gattu *et al.* [49] which also studies the CF description of LDOS of FQH states.

Acknowledgments. We thank Y.-H. Wu for useful discussions. We acknowledge support from Leverhulme Trust Research Leadership Award No. RL-2019-015 and Royal Society International Exchanges Grant No. IES/R2/202052. This research was supported in part by NSF Grants No. PHY-1748958 and No. PHY-2309135 to the Kavli Institute for Theoretical Physics (KITP). N.R. acknowledges support from the QuantERA II Programme, which has received funding from the European Union's Horizon 2020 research and innovation program under Grant Agreement No. 101017733. Computational portions of this research work were carried out on ARC3 and ARC4, part of the High-Performance Computing facilities at the University of Leeds, United Kingdom, and the Nandadevi supercomputer, which is maintained and supported by the Institute of Mathematical Science's High-Performance Computing Center. Some of the numerical calculations were performed using the DIAGHAM package [50]. A.C.B. thanks the Science and Engineering Research Board (SERB) of the Department of Science and Technology (DST) for funding support via Mathematical Research Impact Centric Support (MATRICS) Grant No. MTR/2023/000002. A.Y., Y.H., Y.-C.T., and M.H. acknowledge primary support from DOE-BES Grant No. DE-FG02-07ER46419 and the Gordon and Betty Moore Foundation's EPiQS initiative, Grant No. GBMF9469. Other support to A.Y. from NSF-MRSEC through Princeton Center for Complex Materials Grant No. NSF-DMR-2011750, ARO MURI (Grant No. W911NF-21-2-0147), and ONR Grant No. N00012-21-1-2592 is also acknowledged.

[1] D. C. Tsui, H. L. Stormer, and A. C. Gossard, Two-dimensional magnetotransport in the extreme quantum limit, Phys. Rev. Lett. **48**, 1559 (1982).

[2] R. B. Laughlin, Anomalous quantum Hall effect: An incompressible quantum fluid with fractionally charged excitations, Phys. Rev. Lett. **50**, 1395 (1983).

[3] *The Quantum Hall Effect*, edited by R. E. Prange and S. M. Girvin (Springer, New York, 1987).

[4] *Perspectives in Quantum Hall Effects*, edited by S. Das Sarma and A. Pinczuk (Wiley-VCH, Weinheim, 2007).

[5] B. Halperin and J. Jain, *Fractional Quantum Hall Effects: New Developments* (World Scientific, Singapore, 2020).

[6] J. Nakamura, S. Liang, G. C. Gardner, and M. J. Manfra, Direct observation of anyonic braiding statistics, Nat. Phys. **16**, 931 (2020).

[7] R. L. Willett, K. Shtengel, C. Nayak, L. N. Pfeiffer, Y. J. Chung, M. L. Peabody, K. W. Baldwin, and K. W. West, Interference measurements of non-Abelian $e/4$ & Abelian $e/2$ quasiparticle braiding, Phys. Rev. X **13**, 011028 (2023).

[8] X. Liu, G. Farahi, C.-L. Chiu, Z. Papic, K. Watanabe, T. Taniguchi, M. P. Zaletel, and A. Yazdani, Visualizing broken symmetry and topological defects in a quantum Hall ferromagnet, Science **375**, 321 (2022).

[9] A. Coissard, D. Wander, H. Vignaud, A. G. Grushin, C. Repellin, K. Watanabe, T. Taniguchi, F. Gay, C. B. Winkelmann, H. Courtois, H. Sellier, and B. Sacépé, Imaging tunable quantum Hall broken-symmetry orders in graphene, Nature (London) **605**, 51 (2022).

[10] G. Farahi, C.-L. Chiu, X. Liu, Z. Papic, K. Watanabe, T. Taniguchi, M. P. Zaletel, and A. Yazdani, Broken symmetries and excitation spectra of interacting electrons in partially filled Landau levels, Nat. Phys. **19**, 1482 (2023).

[11] Y. Hu, Y.-C. Tsui, M. He, U. Kamber, T. Wang, A. S. Mohammadi, K. Watanabe, T. Taniguchi, Z. Papic, M. P. Zaletel, and A. Yazdani, High-resolution tunneling spectroscopy of fractional quantum Hall states, arXiv:2308.05789.

[12] R. C. Ashoori, J. A. Lebens, N. P. Bigelow, and R. H. Silsbee, Equilibrium tunneling from the two-dimensional electron gas in GaAs: Evidence for a magnetic-field-induced energy gap, Phys. Rev. Lett. **64**, 681 (1990).

[13] J. P. Eisenstein, L. N. Pfeiffer, and K. W. West, Coulomb barrier to tunneling between parallel two-dimensional electron systems, Phys. Rev. Lett. **69**, 3804 (1992).

[14] O. E. Dial, R. C. Ashoori, L. N. Pfeiffer, and K. W. West, High-resolution spectroscopy of two-dimensional electron systems, Nature (London) **448**, 176 (2007).

[15] O. E. Dial, R. C. Ashoori, L. N. Pfeiffer, and K. W. West, Anomalous structure in the single particle spectrum of the fractional quantum Hall effect, Nature (London) **464**, 566 (2010).

[16] H. M. Yoo, K. W. Baldwin, K. West, L. Pfeiffer, and R. C. Ashoori, Spin phase diagram of the interacting quantum Hall liquid, Nat. Phys. **16**, 1022 (2020).

[17] X. Du, I. Skachko, F. Duerr, A. Luican, and E. Y. Andrei, Fractional quantum Hall effect and insulating phase of Dirac electrons in graphene, Nature (London) **462**, 192 (2009).

[18] K. Bolotin, F. Ghahari, M. D. Shulman, H. Stormer, and P. Kim, Observation of the fractional quantum Hall effect in graphene, Nature (London) **462**, 196 (2009).

[19] C. R. Dean, A. F. Young, P. Cadden-Zimansky, L. Wang, H. Ren, K. Watanabe, T. Taniguchi, P. Kim, J. Hone, and K. L. Shepard, Multicomponent fractional quantum Hall effect in graphene, Nat. Phys. **7**, 693 (2011).

[20] B. E. Feldman, B. Krauss, J. H. Smet, and A. Yacoby, Unconventional sequence of fractional quantum Hall states in suspended graphene, Science **337**, 1196 (2012).

[21] A. Kou, B. E. Feldman, A. J. Levin, B. I. Halperin, K. Watanabe, T. Taniguchi, and A. Yacoby, Electron-hole asymmetric integer and fractional quantum Hall effect in bilayer graphene, Science **345**, 55 (2014).

[22] D.-K. Ki, V. I. Fal'ko, D. A. Abanin, and A. F. Morpurgo, Observation of even denominator fractional quantum Hall effect in suspended bilayer graphene, Nano Lett. **14**, 2135 (2014).

[23] P. Maher, L. Wang, Y. Gao, C. Forsythe, T. Taniguchi, K. Watanabe, D. Abanin, Z. Papić, P. Cadden-Zimansky, J. Hone, P. Kim, and C. R. Dean, Tunable fractional quantum Hall phases in bilayer graphene, Science **345**, 61 (2014).

[24] F. Amet, A. J. Bestwick, J. R. Williams, L. Balicas, K. Watanabe, T. Taniguchi, and D. Goldhaber-Gordon, Composite fermions and broken symmetries in graphene, Nat. Commun. **6**, 5838 (2015).

[25] A. Luican-Mayer, M. Kharitonov, G. Li, C.-P. Lu, I. Skachko, A.-M. B. Gonçalves, K. Watanabe, T. Taniguchi, and E. Y. Andrei, Screening charged impurities and lifting the orbital degeneracy in graphene by populating Landau levels, Phys. Rev. Lett. **112**, 036804 (2014).

[26] B. E. Feldman, M. T. Randeria, A. Gyenis, F. Wu, H. Ji, R. J. Cava, A. H. MacDonald, and A. Yazdani, Observation of a nematic quantum Hall liquid on the surface of bismuth, Science **354**, 316 (2016).

[27] J. K. Jain, Composite-fermion approach for the fractional quantum Hall effect, Phys. Rev. Lett. **63**, 199 (1989).

[28] E. H. Rezayi, Electron and quasiparticle density of states in the fractionally quantized Hall effect, Phys. Rev. B **35**, 3032 (1987).

[29] S. He, P. M. Platzman, and B. I. Halperin, Tunneling into a two-dimensional electron system in a strong magnetic field, Phys. Rev. Lett. **71**, 777 (1993).

[30] R. Haussmann, H. Mori, and A. H. MacDonald, Correlation energy and tunneling density of states in the fractional quantum Hall regime, Phys. Rev. Lett. **76**, 979 (1996).

[31] A. H. MacDonald, Theory of high-energy features in the tunneling spectra of quantum-Hall systems, Phys. Rev. Lett. **105**, 206801 (2010).

[32] L.-K. Lim, M. O. Goerbig, and C. Bena, Theoretical analysis of the density of states of graphene at high magnetic fields using Haldane pseudopotentials, Phys. Rev. B **84**, 115404 (2011).

[33] G. Chaudhary, D. K. Efimkin, and A. H. MacDonald, Tunneling density of states, correlation energy, and spin polarization in the fractional quantum Hall regime, Phys. Rev. B **100**, 085107 (2019).

[34] F. D. M. Haldane, Fractional quantization of the Hall effect: A hierarchy of incompressible quantum fluid states, Phys. Rev. Lett. **51**, 605 (1983).

[35] J. K. Jain and M. R. Peterson, Reconstructing the electron in a fractionalized quantum fluid, Phys. Rev. Lett. **94**, 186808 (2005).

[36] J. K. Jain, *Composite Fermions* (Cambridge University Press, New York, 2007).

[37] Z. Papić, R. S. K. Mong, A. Yazdani, and M. P. Zaletel, Imaging anyons with scanning tunneling microscopy, Phys. Rev. X **8**, 011037 (2018).

[38] S. Pu, A. C. Balram, and Z. Papić, Local density of states and particle entanglement in topological quantum fluids, Phys. Rev. B **106**, 045140 (2022).

[39] S. S. Mandal and J. K. Jain, Theoretical search for the nested quantum Hall effect of composite fermions, Phys. Rev. B **66**, 155302 (2002).

[40] See Supplemental Material at http://link.aps.org/supplemental/10.1103/PhysRevB.110.L081107 for detailed information about the wave functions, diagonalizations, a toy model for the LDOS peak amplitudes, comparison between exact diagonalizations and CF results, the particle side of $\nu = 3/7$, which includes Refs. [51–59].

[41] A. C. Balram, A. Wójs, and J. K. Jain, State counting for excited bands of the fractional quantum Hall effect: Exclusion rules for bound excitons, Phys. Rev. B **88**, 205312 (2013).

[42] G. J. Sreejith, Y.-H. Wu, A. Wójs, and J. K. Jain, Tripartite composite fermion states, Phys. Rev. B **87**, 245125 (2013).

[43] A. C. Balram, A non-Abelian parton state for the $\nu = 2 + 3/8$ fractional quantum Hall effect, SciPost Phys. **10**, 83 (2021).

[44] G. Dev and J. K. Jain, Band structure of the fractional quantum Hall effect, Phys. Rev. Lett. **69**, 2843 (1992).

[45] X. G. Wu and J. K. Jain, Excitation spectrum and collective modes of composite fermions, Phys. Rev. B **51**, 1752 (1995).

[46] N. d'Ambrumenil and R. Morf, Hierarchical classification of fractional quantum Hall states, Phys. Rev. B **40**, 6108 (1989).

[47] A. C. Balram, Z. Liu, A. Gromov, and Z. Papić, Very-high-energy collective states of partons in fractional quantum Hall liquids, Phys. Rev. X **12**, 021008 (2022).

[48] D. X. Nguyen, F. D. M. Haldane, E. H. Rezayi, D. T. Son, and K. Yang, Multiple magnetorotons and spectral sum rules in fractional quantum Hall systems, Phys. Rev. Lett. **128**, 246402 (2022).

[49] M. Gattu, G. J. Sreejith, and J. K. Jain, Scanning tunneling microscopy of fractional quantum Hall states: Spectroscopy of composite-fermion bound states, Phys. Rev. B **109**, L201123 (2024).

[50] DIAGHAM, https://www.nick-ux.org/diagham.

[51] T. T. Wu and C. N. Yang, Dirac monopole without strings: Monopole harmonics, Nucl. Phys. B **107**, 365 (1976).

[52] J. K. Jain and R. K. Kamilla, Composite fermions in the Hilbert space of the lowest electronic Landau level, Int. J. Mod. Phys. B **11**, 2621 (1997).

[53] J. K. Jain and R. K. Kamilla, Quantitative study of large composite-fermion systems, Phys. Rev. B **55**, R4895(R) (1997).

[54] A. C. Balram, C. Töke, A. Wójs, and J. K. Jain, Phase diagram of fractional quantum Hall effect of composite fermions in multicomponent systems, Phys. Rev. B **91**, 045109 (2015).

[55] R. H. Morf, N. d'Ambrumenil, and S. Das Sarma, Excitation gaps in fractional quantum Hall states: An exact diagonalization study, Phys. Rev. B **66**, 075408 (2002).

[56] A. C. Balram and S. Pu, Positions of the magnetoroton minima in the fractional quantum Hall effect, Eur. Phys. J. B **90**, 124 (2017).

[57] T. Zhao, K. Kudo, W. N. Faugno, A. C. Balram, and J. K. Jain, Revisiting excitation gaps in the fractional quantum Hall effect, Phys. Rev. B **105**, 205147 (2022).

[58] R. Morf, N. d'Ambrumenil, and B. I. Halperin, Microscopic wave functions for the fractional quantized Hall states at $\nu = \frac{2}{5}$ and $\frac{2}{7}$, Phys. Rev. B **34**, 3037 (1986).

[59] A. Weiße, G. Wellein, A. Alvermann, and H. Fehske, The kernel polynomial method, Rev. Mod. Phys. **78**, 275 (2006).